A Venturini based Modulation Technique for a New Isolated AC/AC Power Converter

Usman Nasir[1], Marco Rivera[2], Alessandro Costabeber [1] and Patrick Wheeler [1]
[1] The University of Nottingham, UK
[2] Universidad de Talca, Chile
[1] usman.nasir@nottingham.ac.uk, [2] marcoriv@utalca.cl

***Abstract*— The Future Global Electricity Network is expected to have large integration of renewable generators, and to be widely interconnected. As a consequence, the multi-modular bidirectional AC/AC power conversion architectures will play a major role in improving power flow controllability, power quality and availability. This paper proposes a new power converter topology suitable for AC/AC conversion in medium and high voltage applications, based on the matrix concept. The proposed topology combines the advantages of matrix converters with those of modular converters, providing high modularity and scalability, reduced weight and volume, minimum number of conversion stages and minimum energy storage. Galvanic isolation is provided at medium frequency, reducing size and cost of the transformer. The paper introduces the converter concept and commutation strategy and proposes a modified Venturini modulation in order to provide a per-switching cycle control of the Volt-Second balance across the transformer.**

Keywords—isolated AC/AC; Venturini Modulation; cycloconverter; 4-step commutation; Voltage-Time Balance

I. INTRODUCTION

Matrix converters offer a compact and high power density AC/AC conversion solution avoiding large capacitive energy storage [1]. However, classic matrix converters are not a viable solution in applications requiring galvanic isolation. If the AC/AC conversion unit is intended for the inter-connection of AC transmission or distribution grids, the converter must include an isolation stage [2] to minimize the impact of a fault on the semiconductors and to prevent the fault propagation through the system. The scenario can be worse for converters with a significantly large number of devices such as modular multilevel converters [2]. Employing a line frequency transformer can provide isolation but results in high cost and large volume and weight [3, 4], and especially in applications where cost is a relevant constraint, such as medium voltage distribution systems, a Medium Frequency (MF) transformer is normally preferred.

In addition to the conventional AC/DC/MF/DC/AC architecture [2], an alternative configuration for isolated AC/AC converters is a direct AC/MF/AC architecture based on the matrix concept, that avoids the intermediate AC/DC conversion stages and eliminates the need for large energy storage within the converter. Some aspects related with control and modulation of an AC/MF/AC have been provided in [5-9] for a single-phase to single-phase converter. Nevertheless, the case where the output frequency of the converter is different from the input frequency, has not been addressed. Moreover, any variation in the input frequency will be reflected at the output side. The main drawback of the solutions proposed in [5-9] is its limited application and this is mainly due to the single-phase to single phase nature of the converter. Hence, a modification in the topology is required to exploit the AC/MF/AC direct conversion concept and extend the range of applicability while maintaining the constraints [2] such as modularity and flexibility. The topology proposed in this paper extends the original concept to a three-phase to single-phase converter first, shown in Fig. 1, and then to a complete three-phase to three-phase system. The major advantages of the proposed solution are:

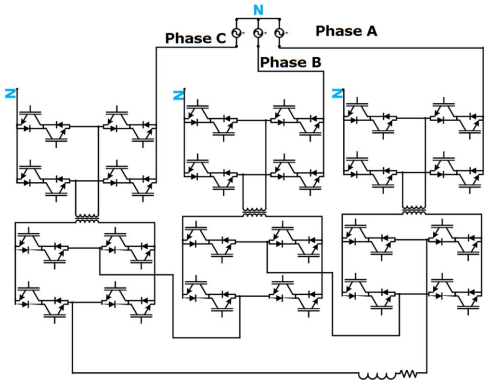

Fig. 1 The proposed isolated AC/AC three phase to single phase topology using three Dual CBM

- *Reduced number of conversion stages compared to isolated AC/DC/DC/AC configurations.*
- *Modular and flexible structure, that can be adapted to different power/voltage levels (not shown in figure, but the series connection of a larger numbers of modules provides voltage scalability).*
- *Absence of large energy storage components i.e. DC link capacitors.*
- *Improved spectrum of output phase voltages compared to the single-phase to single-phase solution.*

Section II discusses the limitations of the single-phase to single-phase solutions [5-9] and the evolution into the new proposed topology. Section III proposes a possible modulation and commutation methodology for the new topology, including a Volt-Second balancing scheme for the transformer. Section IV extends the analysis to the three-phase to three-phase topology. Section V presents time-domain simulation results in Plecs, validating the proposed concepts and confirming the potential of the new topology.

This publication was made possible by the Fondecyt Regular Project N 1160690, the Newton Picarte Project EPSRC: EP/N004043/1: New Configurations of Power Converters for Grid Interconnection Systems/ CONICYT DPI20140007.

II. Background

A. Existing Single-Phase To Single-Phase AC/AC Converters

Focusing on single-phase to single phase topologies, [5-9] proposed a new family of current-mode and voltage mode converters, suitable for AC/AC conversion including MF isolation transformer.

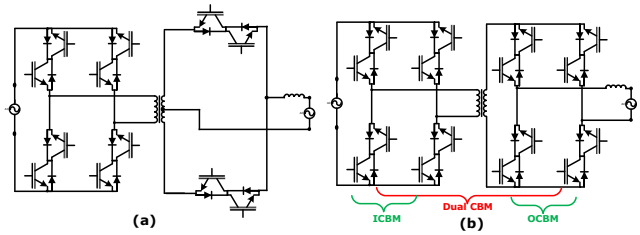

Fig. 2 (a) An isolated AC/AC full bridge full wave converter (b) An isolated AC/AC dual cycloconverter based module (Dual CBM)

Within the sub-family of voltage mode converters, the topology shown in Fig. 2 (b) and defined in literature as *'full bridge-full bridge mode'*, is particularly attractive for grid applications, being highly modular – the converter is made by the interconnection of two identical bridges to the MF transformer - and this feature enhances manufacturing and simplified converter deployment especially in medium and high voltage applications. In the following analysis, this converter will be referred as Dual Cycloconverter Based Module (Dual-CBM)[10], to highlight its inherent modularity.

Despite the large amount of information provided by [6]-[9], detailed analysis is provided only for a simplified version of the converter, referred as *'full bridge- full wave mode'* and shown in Fig. 2 (a). Experimental results are provided for the CBM, but are not completely supported by a theoretical analysis. In addition, the existing contributions address the operation of the converter when feeding a local load, and low voltage low power applications are targeted.

One of the main drawbacks, using single cell, is its limitation to applications in which the output frequency is same as the output frequency. However, by modifying the modulation, it is only possible to generate the integral multiples of the input frequency at the output. For instance, with the single cell converter of [6]-[9], it is impossible to generate 50Hz output from 60Hz input. Therefore, the single cell will fail to interconnect AC networks at different frequencies i.e. 50-60 Hz.

B. Proposed solution : new AC/AC topology

Intuitively, the reason why the Dual-CBM fail when the output frequency is different from input, is that the voltage that can be generated at the output is limited by the instantaneous value of the input voltage. Moving from a single-phase to single-phase converter to the three-phase to single-phase in Fig. 1, the three phase input gives the converter a range of input options to be selected for a specific desired output voltage waveform. Considering the output 'phase a', at any time instant the matrix converter can select either 'phase A', 'phase B' or 'phase C', resulting in higher output voltage controllability and smaller filter. This comes at the cost of increased number of semiconductors, but the higher degree of modularity is expected to compensate for it.

The new converter generates each output phase to neutral voltage with the series connection of three Dual-CBMs, each of them connected to one of the input phases. This maximizes the output voltage generation capacity, reducing at the same time the filtering requirements. Suitable commutation modulation strategies must be developed for the new converter, as discussed in the following section.

It is important to mention that the voltage across the transformer needs to be in MF range. Therefore, in order to change the polarity of voltage across the MF transformer, only those states will be utilized which change the voltage polarity at transformer without affecting the output voltage polarity i.e. moving between state 1 and state 2. Therefore, standard modulation techniques can be applied. See Fig. 3.

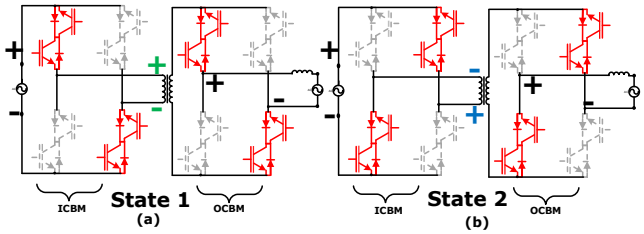

Fig. 3 Active states of Dual-CBM (a) State 1: Voltage polarity at transformer is same as input voltage (b) State 2: Voltage polarity at transformer is opposite to input voltage

III. Commutation And Modulation Strategy For New Isolated AC/AC Topology

Since the new AC/AC isolated topology is based on the matrix conversion concept, modulation and commutation strategy should be developed in accordance with the matrix converters operating principles.

A. Commutation Strategy

1) Commutation of Dual Cycloconverter Based Module (Dual-CBM)

A possible commutation strategy for the OCBM can be developed starting from the 4-step commutation for standard matrix converters. Due to the higher complexity of the new AC/AC isolated topology, a new dedicated procedure must be developed, both for current based and voltage based commutation. The same commutation method is also applicable to ICBM.

a) Output Current Based Commutation

In the current based commutation, the output current is sensed and based on its direction, the commutation process is initiated. During the commutation, it is assumed that the current direction does not change. Based on the operating principle, the OCBM has three steady states i.e. positive, zero or negative which are shown in Fig. 4(a), Fig. 4(e) and Fig. 4(i), respectively. A generalized path for moving from positive to zero and then to negative has been shown in Fig. 4. A shorter path, when moving directly from positive to negative, is possible by avoiding intermediate zero states i.e. states 5 and 6 of Fig. 4(e) and Fig. 4(f), respectively. Note that this is true for the voltage based commutation as well.

The proposed procedure, illustrated in Fig. 4, is as follows:

State 1) At $t=t_1$ the converter is in steady state 1 with **s1o, s0o, s3o, s2o** in **on state**. The current direction has been assumed as shown in Fig. 4(a), i.e. $\mathbf{I_o>0}$.

State 2) At $t=t_2$,with $I_o>0$, the switches **s1o** and **s3o** are not conducting and can be **turned off**. In this state, only two switches i.e. **s0o, s2o** are on in **on state** as shown in Fig. 4(b).

State 3) At $t=t_3$, as s1o is now turned off, the switch **s7o** can be **turned on** safely i.e. V_{in} is not short circuited. Three switches i.e. **s0o, s2o, s7o** are in **on state** as shown in Fig. 4(c).

State 4) At $t=t_4$, the switch **s0o** is **turned off** because s7o is in on state. In this state, only two switches i.e. **s2o, s7o** are in **on state** as shown in Fig. 4(d).

State 5) At $t=t_5$, in order to allow the converter to conduct for $I_o<0$ as well, the switches **s6o, s3o** are **turned on**. Therefore, the converter reaches its steady state 2 as shown in Fig. 4(e) which is a zero state.

State 6) At $t=t_6$, with $I_o>0$, the switches **s6o, s3o** are not conducting and can be **turned off.** In this state, only two switches i.e. **s2o, s7o** are in **on state** as shown in Fig. 4(f).

State 7) At $t=t_7$, the switch **s5o** can be **turned on** safely i.e. V_{in} is not short circuited. In this state, three switches i.e. **s0o, s2o, s5o** are in **on state** as shown in Fig. 4(g).

State 8) At $t=t_8$, the switch **s2o** is **turned off** because the switch s5o is in on state. In this state, only two switches i.e. **s5o, s7o** are in **on state** as shown in Fig. 4(h).

State 9) At $t=t_9$, in order to allow the converter to conduct for $I_o<0$ as well, the switches **s4o, s6o** are **turned on**. The converter is in steady state 3 with **s4o, s5o, s6o, s7o** in **on state** as shown in Fig. 4(i).

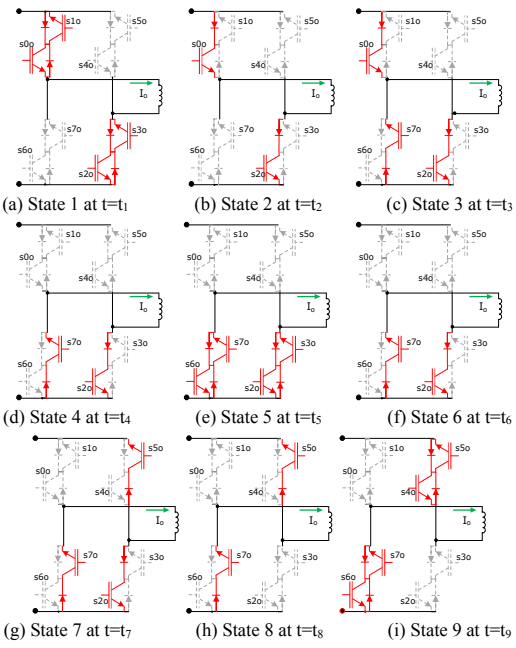

(a) State 1 at $t=t_1$ (b) State 2 at $t=t_2$ (c) State 3 at $t=t_3$

(d) State 4 at $t=t_4$ (e) State 5 at $t=t_5$ (f) State 6 at $t=t_6$

(g) State 7 at $t=t_7$ (h) State 8 at $t=t_8$ (i) State 9 at $t=t_9$

Fig. 4 States for output current based commutation method for the Output Cycloconverter Based Module (OCBM)

b) Input Voltage Based Commutation

In the voltage based commutation, based on the sign of the voltage, the commutation process is initiated. The proposed procedure, illustrated in Fig. 5, is as follows:

State 1) At $t=t_1$ the converter is in steady state 1 with **s1o, s0o, s3o, s2o** in **on state**. The sign of voltage has been assumed as shown in Fig. 5(a), i.e. $\mathbf{V_{in}>0}$.

State 2) At $t=t_2$, with $V_{in}>0$, the switch **s7o** can be **turned on** safely. In this state, five switches i.e. **s1o s2o, s3o, s6o, s7o** are in **on state** as shown in Fig. 5(b).

State 3) At $t=t_3$, the switch **s0o** has been **turned off** because the switch s7o is in on state. In this state, four switches i.e. **s1o, s2o, s3o, s7o** are in **on state** as shown in Fig. 5(c).

State 4) At $t=t_4$, the switch **s6o** can be **turned on** safely. In this state, five switches i.e. **s0o, s1o s2o, s3o, s7o** are in **on state** as shown in Fig. 5(d).

State 5) At $t=t_5$ the switch **s1o** is **turned off** because the switch s6o is in on state. In this state, four switches i.e. **s2o, s3o, s6o, s7o** are in on state. Therefore, the converter reaches its steady state 2 as shown in Fig. 5(e) which is a zero state.

State 6) At $t=t_6$, the switch **s5o** can be **turned on** safely. In this state, five switches i.e. **s2o, s3o, s5o, s6o, s7o** are in **on state** as shown in Fig. 5(f).

State 7) At $t=t_7$, the switch **s2o** is **turned off** because the switch s5o is in on state. In this state, four switches i.e. **s3o, s5o, s6o, s7o** are in **on state** as shown in Fig. 5(g).

State 8) At $t=t_8$, the switch **s4o** can be **turned on** safely. In this state, five switches i.e. **s3o s4o, s5o, s6o, s7o** are in **on state** as shown in Fig. 5(h).

State 9) At $t=t_9$, with $V_{in}>0$, the switch **s3o** is **turned off** because the switch s4o can also conduct for $I_o<0$. In this state, four switches i.e. **s4o, s5o, s6o, s7o** are in on state. Therefore, the converter reaches its steady state 3 as shown in Fig. 5(i).

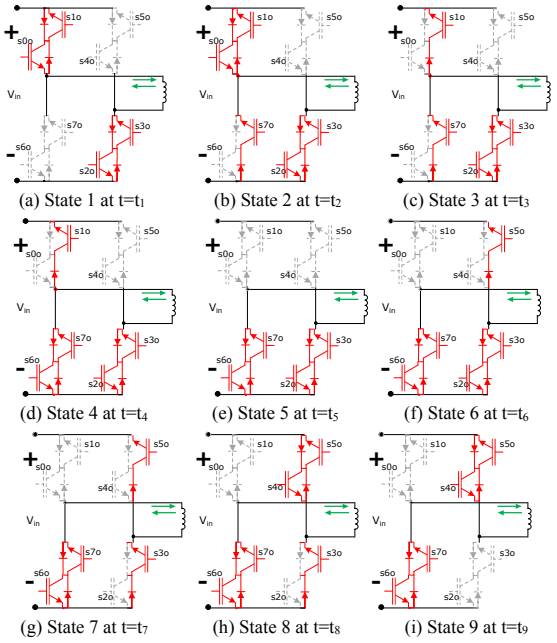

(a) State 1 at $t=t_1$ (b) State 2 at $t=t_2$ (c) State 3 at $t=t_3$

(d) State 4 at $t=t_4$ (e) State 5 at $t=t_5$ (f) State 6 at $t=t_6$

(g) State 7 at $t=t_7$ (h) State 8 at $t=t_8$ (i) State 9 at $t=t_9$

Fig. 5 States for input votlage based commutation method of output cycloconverter based module (OCBM)

B. *Venturini Modulation Method*

The 'Venturini Modulation Method' was presented by M. Venturini and A. Alesina in 1980 [11] for the direct matrix converter shown in Fig. 6. In average terms, the output voltage is related to the input voltage as:

$$[v_o(t)] = [M(t)][v_i(t)] \quad (1) \qquad \begin{bmatrix} v_a(t) \\ v_b(t) \\ v_c(t) \end{bmatrix} = \begin{bmatrix} m_{Aa}(t) & m_{Ba}(t) & m_{Ca}(t) \\ m_{Ab}(t) & m_{Bb}(t) & m_{Cb}(t) \\ m_{Ac}(t) & m_{Bc}(t) & m_{Cc}(t) \end{bmatrix} \begin{bmatrix} v_A(t) \\ v_B(t) \\ v_C(t) \end{bmatrix} \quad (2)$$

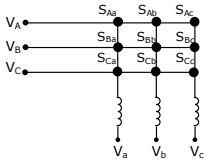

Fig. 6 A direct matrix converter with 9 bidirectional switches

Where m_{Kj} are is the generic modulation index for the switch in position Kj. The constraint on the switches i.e. input voltage source cannot be short circuited and output current source cannot be opened, can be expressed by (3).

$$\sum_{K=A,B,C} S_{Ka}(t) = \sum_{K=A,B,C} S_{Kb}(t) = \sum_{K=A,B,C} S_{Kc}(t) = 1 \quad (3)$$

By solving (1) and (3) for the unity input displacement factor, the corresponding modulation function can be expressed by a simplified form in (4). Where $K=A,B,C$ and $j=a,b,c$. For instance, when $K=A$ and $j=a$, then from (4), the time can be represented as in (5).

$$m_{Kj} = \frac{1}{3}\left(1 + \frac{2v_K v_j}{{V_m}^2}\right) \quad (4)$$

$$t_{Aa} = \frac{T_S}{3}(1 + 2q\cos(\omega_i t)\cos(\omega_o t)) \quad (5)$$

Where t_{Aa}=Turn on time of S_{Aa} i.e to connect output phase a with input phase A. In order to apply the matrix converter's modulation techniques to the topology under study, one way is to consider the switching pattern shown in Fig. 7 and the illustration has only been given for t_{Aa}. The following parameters have been considered for the simulation, based on a low voltage setup suitable for laboratory scale experimental validation.

TABLE I. SIMULATION PARAMETERS

Parameter	Value
Input voltage V_{in}	220V AC
Voltage regulation ratio q	0.5
[a]Input frequency f_{in}	50 Hz
Output demanded frequency f_o	40 Hz
ICBM switching frequency f_{Trans}	2kHz
Output Load	R=1 Ω,L=1 mH

[a]. Changed from 50 Hz to 86 Hz for test

It must be noted that during the time t_{Aa}, only Phase A is required while the other two phases i.e. phases B and C are not required at the output. So, in the OCBMs of the other two phases, two upper or two lower bidirectional switches are closed and bypasses the transformer [12] which can help to decrease the overall conduction losses. From Fig. 7 as the OCBMs are series connected, therefore the individual output voltages of the OCBMs are summed up to form the output load voltage which is similar to a traditional matrix converter as shown in Fig. 9. In this kind of modulation, the converter regulates the output reference frequency, i.e. 40Hz, regardless of variation in the frequency of three phase input. As shown in Fig. 8, even an exaggerated change in the input frequency from 50Hz to 86Hz is not affecting the fundamental component of output voltage and current.

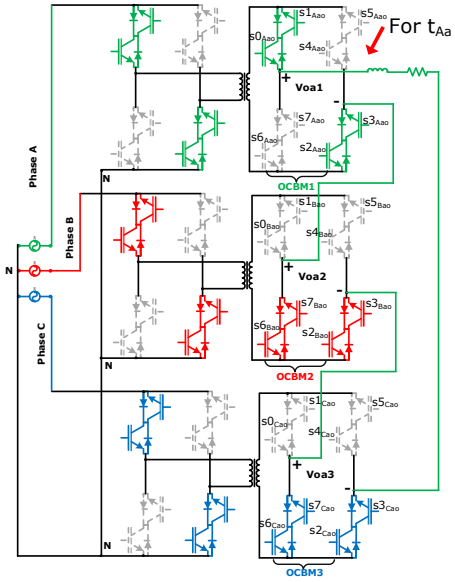

Fig. 7 Application of the turn on time t_{Aa} obtained from Venturini Modulation to the new isolated AC/AC topology

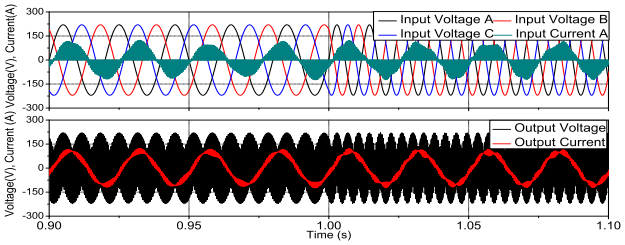

Fig. 8 Output frequency regulation at 40Hz regardless of the input frequency change, i.e 50-86 Hz, applied at time=1s

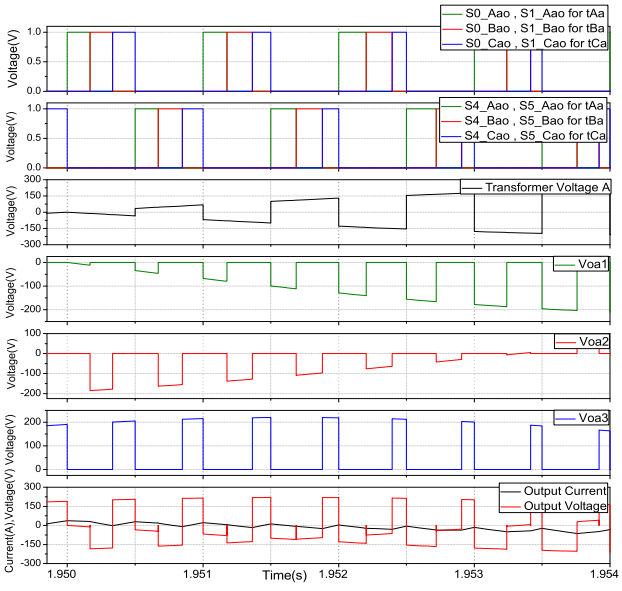

Fig. 9 Gating signals for the OCBMs and their respective output voltages in the new isolated 3-Phase to 1-Phase AC/AC topology

1) Volt-Second Balance across MF Transformer

a) Saturation Control

An active control of the Volt-Second balance across the transformer is mandatory in order to avoid saturation of the core due to undesired DC components generated by converter asymmetries – e.g. differences in the turn on/off times of switches, gate driver delays etc. The voltage based control loop of Fig. 10 has been considered to introduce the control concept. The control loop extracts the DC component of the voltage with a low pass filter and modifies the switching time *t* by an amount of *Δt*, such that the DC component over the voltage period T is set to zero. This modification of switching time will not affect the modulation as the converter moves between State 1 and 2 of Fig. 3. Note that this is shown in this form only to highlight the control capability achieved modifying switching times.

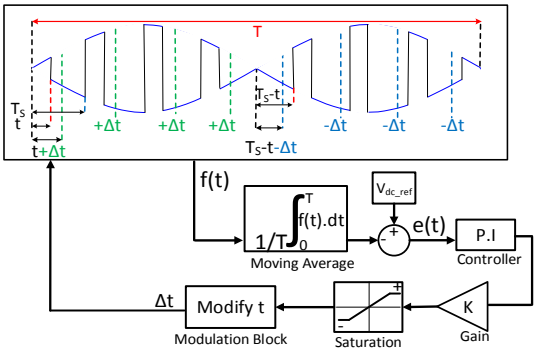

Fig. 10 Voltage based closed loop controller for voltage-time balance of transformer

Since the final output of this control has to be time i.e. *Δt*, therefore a gain and a saturation block is necessary to limit *Δt*. Limits of saturation need careful attention, with T_S=1ms and t=0.5ms, the upper and lower limit must be less than 0.5ms. From Fig. 10, if *Δt>0*, then overall dc component of the wave will tend to a positive value and if *Δt<0*, the overall dc component will tend to a negative value. Therefore, voltage polarity at transformer is now to be changed, by moving between the states of Fig. 3, at the new time *t* i.e *t+Δt*.

The values *'kp'* and *'ki'* of P.I controller have been estimated using Ziegler–Nichols method. In order to verify this control loop, a delay in the switching time *t* is introduced to model a turn-on delay and from Fig. 11 it can be seen that error *e(t)* in the DC component of the proposed closed loop becomes zero in comparison to open loop system.

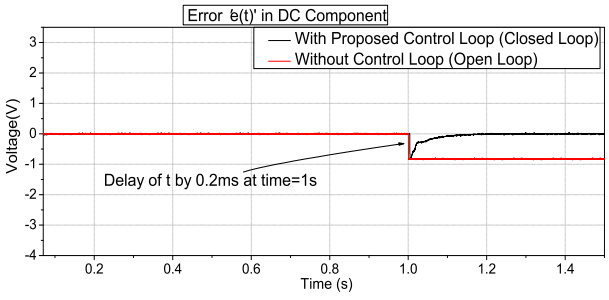

Fig. 11 Response of error 'e(t)' of dc component of votlage in case of open and closed loop system when the switching time *t* is delayed by a value of 0.2ms at time=1s.

b) Per-Switching Cycle Feed Forward Compensation

The proposed closed loop control is acting on the fundamental period of input voltage i.e. T but it is also possible to add a feed forward compensation which can help to minimize the per-switching-cycle flux variation, eventually decreasing the core size of transformer and reducing loss. From Fig. 12, the average over the first switching cycle of the transformer's voltage can be found using (6).

$$a_0 = \frac{1}{\omega T_S}\left[\int_0^t V_m \sin(\omega t).\,dt + \int_t^{T_S} -V_m \sin(\omega t).\,dt\right] \quad (6)$$

$$a_0 = \frac{T.V_m}{2\pi.T_S}[1 - 2\cos(\omega t) + \cos(\omega TS)] \quad (7)$$

Where;
V_m=Amplitude of Input Voltage=220V, T=Fundamental Period of Voltage=20ms
ω=Angular Frequency=2π/T, T_S=Switching Period=1ms, t=T_S/2=0.5ms

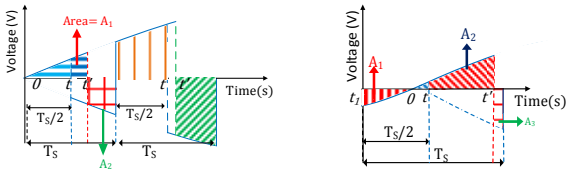

Fig. 12 (a) Selection of switching time *t'* to achieve ZASC (b) Selection of *t'* to achieve ZASC when the phase of the input votlage is non-zero.

The average over the first switching cycle is found out to be 17.02V which is 7.74% of the input voltage amplitude. Similarly, for the second switching cycle it is 15.36V i.e. 6.983% of the input voltage amplitude. Therefore, average over each of the switching cycles is different and a generalized expression to calculate average of n^{th} switching cycle has been found (8).

$$a_0 = \frac{T.V_m}{2\pi.T_S}\left[(\cos(\omega T_S(n-1)) - 2\cos\left(\omega T_S(n-\tfrac{1}{2})\right) + \cos(n\omega T_S))\right] \quad (8)$$

Where n=Number of Switching Cycle *For 1st cycle n=1

In order to ensure that there is Zero Average over each Switching Cycle (ZASC), the following method has been developed. From Fig. 12, area under the curve from *0* to *t'* i.e. A_1 and area from *t'* to T_S i.e. A_2 can be found by (9) and (10), respectively. Therefore, to achieve ZASC, *t'* must be selected such that the area A_1 equals A_2. Hence, by equating (9) and (10), *t'* can be represented as in (11).

$$A_1 = \int_0^{t'} \sin(\omega t)\,dt \quad (9), \qquad A_2 = \int_{t'}^{TS} \sin(\omega t)\,dt \quad (10)$$

$$t' = \frac{\cos^{-1}(0.5+0.5\cos(\omega TS))}{\omega} \quad (11)$$

Fig. 12 (a) is a simplified case when the input voltage has zero phase but for the case when the input voltage has a non-zero phase, as shown in Fig. 12 (b), the value of time *t'* can be calculated by using. (15).

$$A_1 = \int_0^{t_1} \sin(\omega t)\,dt(12), A_2 = \int_0^{t'} \sin(\omega t)\,dt(13), A_3 = \int_{t'}^{Ts-t1} \sin(\omega t)\,dt(14)$$

$$t' = \frac{\cos^{-1}(0.5\cos(\omega t_1)+0.5\cos(\omega(TS-t1)))}{\omega} + t_1 \quad (15)$$

Therefore, solving (12)-(14) in order to determine *t'* such that it satisfies $A_1+A_3=A_2$ will result in (15). In this case, the information of frequency as well as phase of the input voltage is required to get the value of t_1. This feed forward compensation will not affect the modulation strategy because from Fig. 3, the voltage polarity at transformer can be changed anytime. Now the saturation control with the ZASC will be implemented with the extended three phase to three phase topology.

IV. Extension To A New Three Phase To Three Phase Isolated AC/AC Topology

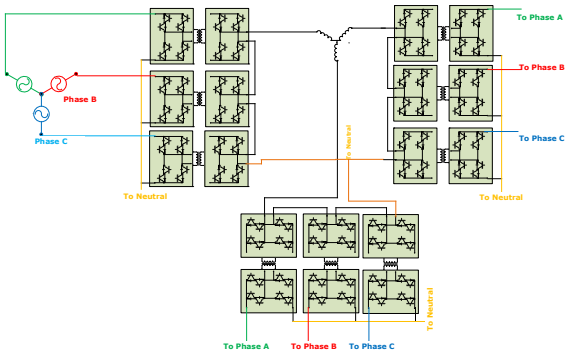

Fig. 13 A new 3-phase to 3-phase isolated AC/AC topology based on 9 Dual CBMs or 18 Bidirectional H-Bridges

The replication of the three-phase to single-phase topology will results in the three-phase to three-phase topology shown in Fig. 13. The simulated three-phase to three-phase system with voltage-time balance is shown in Fig. 15. The FFT of the output voltage, shown in Fig. 14, verifies that the fundamental component of the voltage at 40Hz is in accordance with the 50% Venturini Modulation (VM) Method.

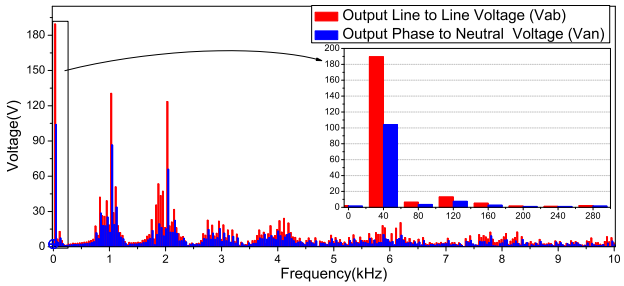

Fig. 14 Comparison of FFT of the line to line with phase to neutral voltage obtained by using Venturini Modulation (VM) method in 3-phase to 3–phase new isolated AC/AC topology with q=0.5

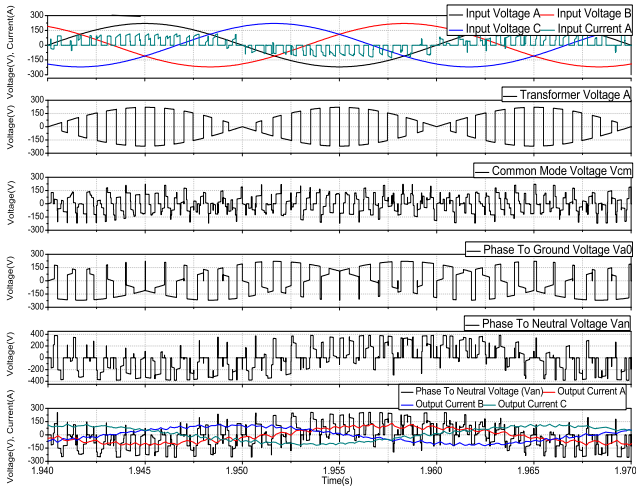

Fig. 15 Venturini Modulation (VM) for the new 3-phase to 3-phase isolated AC/AC topology

V. Conclusion

This paper discussed a new modular and isolated AC/AC conversion topology suitable for grid interconnection. Compared to existing solutions based on single phase to single phase cells, the proposed converter uses the same modular blocks but provides improved voltage generation capability. In particular, input and output frequency decoupling can be achieved making the converter suitable for interconnection of AC grids at different frequencies and the harmonic content of the generated voltage is also improved.

The concept of the proposed converter is the extension of the standard matrix converter to the isolated case. For this reason a suitable Venturini Modulation (VM) Method and 4-Step Commutation Method have been developed and validated in a Plecs simulation. In addition, a transformer saturation controller has been developed. The controller acts on the modulation times and is based on the combination of a slow average controller supported by a per-switching-cycle feed forward compensation that minimizes flux variations.

References

[1] P. Wheeler, J. Clare, L. Empringham, M. Apap, and M. Bland, "Matrix converters," *Power Engineering Journal,* vol. 16, no. 6, pp. 273-282, 2002.

[2] F. B. F. Iov, *Advanced power converters for universal and flexible power management in future electricity network - Converter applications in future European electricity network*, University of Nottingham, School of Electrical and Electronic Engineering, University Park, Nottingham, 2007.

[3] M. D. Manjrekar, R. Kieferndorf, and G. Venkataramanan, "Power electronic transformers for utility applications," in Industry Applications Conference, 2000. Conference Record of the 2000 IEEE, 2000, pp. 2496-2502 vol.4.

[4] H. Yonemori, Y. Nishida, and M. Nakaoka, "New bidirectional sinewave-modulated series resonant power conditioning system with high-frequency AC link," in Telecommunications Energy Conference, 1989. INTELEC '89. Conference Proceedings., Eleventh International, 1989, pp. 14.2/1-14.2/6 vol.2.

[5] L. Lei, and Z. Qinglong, "Comparisons of two kinds of AC/AC converters with high frequency link," in Industrial Electronics, 2008. IECON 2008. 34th Annual Conference of IEEE, 2008, pp. 618-622.

[6] C. Daolian, and L. Lei, "Bi-polarity phase-shifted controlled voltage mode AC/AC converters with high frequency AC link," in Power Electronics Specialist Conference, 2003. PESC '03. 2003 IEEE 34th Annual, 2003, pp. 677-682 vol.2.

[7] C. Daolian, "Novel Current-Mode AC/AC Converters With High-Frequency AC Link," *Industrial Electronics, IEEE Transactions on,* vol. 55, no. 1, pp. 30-37, 2008.

[8] L. Lei, and C. Daolian, "Phase-shifted controlled forward mode AC/AC converters with high frequency AC links," in Power Electronics and Drive Systems, 2003. PEDS 2003. The Fifth International Conference on, 2003, pp. 172-177 Vol.1.

[9] C. Daolian, and L. Jian, "The uni-polarity phase-shifted controlled voltage mode AC-AC converters with high frequency AC link," *Power Electronics, IEEE Transactions on,* vol. 21, no. 4, pp. 899-905, 2006.

[10] D. Siemaszko, F. Zurkinden, L. Fleischli, I. Villar, Y. R. De Novaes, and A. Rufer, "Description and Efficiency Comparison of Two 25 kVA DC/AC Isolation Modules," *EPE Journal,* vol. 19, no. 4, pp. 17-24, 2009/12/01, 2009.

[11] M. Venturini, "A new sine wave in sine wave out conversion technique which eliminates reactive elements." pp. E3_1-E3_15.

[12] C. Zimmermann, A. Rufer, and C. Chabert, "Non-linear properties and efficiency improvements of a bi-directional isolated DC-AC converter with soft commutation," in Industry Applications Conference, 2005. Fourtieth IAS Annual Meeting. Conference Record of the 2005, 2005, pp. 1985-1991 Vol. 3.